Simulation of Lasing Modes in a Kite-Shaped Microcavity Laser

E. I. Smotrova, *Member, IEEE* and A. I. Nosich, *Fellow*, *IEEE*

Institute of Radiophysics and Electronics of National Academy of Sciences of Ukraine, Kharkov, Ukraine

Abstract: We consider the lasing modes in a thin kite-shaped active microcavity as solutions to the 2-D linear eigenproblem for the Maxwell equations with exact boundary and radiation conditions. This problem is reduced to the set of Muller's integral equations with smooth and integrable kernels discretized using the adequate quadrature formulas. The eigenvalues are found numerically as the roots of the corresponding determinantal equation. The results of the study of several modes are presented.

I. INTRODUCTION

A serious drawback of circular microdisk lasers is the low directionality of light emission because any whispering-gallery mode with azimuth index *m* has 2*m* identical beams in the disk plane. Directionality can be conveniently quantified with the aid of *directivity* as a ratio of power emitted into the main beam direction to the total power averaged over all directions. Then any mode of a circular cavity with $m > 0$ has directivity equal to 2. It is evident that improvement of the directionality needs a distortion of the cavity shape from the circle. As such a deformed shape, we will study the kite cavity whose contour can be characterised using a smooth function.

II. EIGENVALUE PROBLEM FOR ACTIVE MICROCAVITIES

Denote the interior domain of a two-dimensional (2-D) model of an active dielectric (non-magnetic) microcavity as D_i, its closed contour as Γ, and the outer domain as D_e. Consider a function $U(x, y)$, which is either the E_z or the H_z field component. When simulating a microlaser, we are interested in real-valued pairs of numbers (k,γ) generating non-zero functions U solving, off Γ, the Helmholtz equation $(\Delta + k^2\nu^2)U = 0$ with a piecewise-constant effective refractive index ν equal to $\nu_i = \alpha_i - i\gamma$ $(\gamma > 0)$ in D_i, and $\nu_e = \alpha_e$ in D_e. Here, the following two-side boundary conditions are required on Γ: $U^e = U^i$ and $\eta_e \partial U^e / \partial n = \eta_i \partial U^i / \partial n$, where the superscripts "i,e" refer to the corresponding domains, $\eta_{i,e} = 1$ (E-polarisation) or $\eta_{i,e} = 1/\nu_{i,e}^2$ (H-polarisation), and $\vec n$ is the outward normal vector to Γ. Furthermore, the time-averaged electromagnetic energy must be locally integrable to prevent source-like field singularities, and the Sommerfeld radiation condition must be satisfied at infinity. This is the Lasing Eigenvalue Problem (LEP) that we have introduced in [1] and systematically used in [2]-[5] to study the modes in various active cavities.

In this paper, we consider a kite-shaped microcavity (Fig.1).

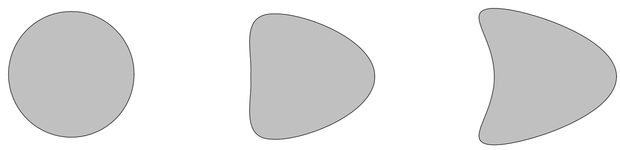

(a) (b) (c)

Fig. 1. Geometries of microcavity for different values of parameter δ: (a) $\delta = 0$, (b) $\delta = 0.3$, (c) $\delta = 0.5$.

For the contour Γ representation, we use the following smooth (i.e. infinitely continuously differentiable) function, where $t \in [0, 2\pi]$:

$$\begin{aligned} &\mathrm{r}(t) = \{x(t), y(t)\}, \\ &x(t) = \cos t + \delta \cos 2t - \delta, \quad y(t) = \sin t \end{aligned} \qquad (1)$$

Here, δ is the contour shape parameter, so that if $\delta = 0$ then (4) turns to a circle. Note that the values of $\delta < 0.29$ provide convex contours and the true kite shape appears only if δ takes larger values.

III. MULLER'S INTEGRAL EQUATIONS

Introduce the Green's functions $G_j(R) = (i/4)H_0^{(1)}(k\nu_j R)$ of the homogeneous media, where $j = i, e$, $R = |\vec r - \vec r'|$ is the distance between the points $\vec r$ and $\vec r'$, and $H_0^{(1)}(\cdot)$ is the Hankel function. After applying the second Green's formula to the functions $G_j(\vec r, \vec r')$ and U_j, using boundary conditions, and taking into account the properties of single-layer and double layer potentials, we obtain two integral equations as

$$\varphi(\vec r) + \int_\Gamma \varphi(\vec r')A(\vec r,\vec r')dl' - \int_\Gamma \psi(\vec r')B(\vec r,\vec r')dl' = 0,$$

$$\frac{\eta_i + \eta_e}{2\eta_e}\psi(\vec r) + \int_\Gamma \varphi(\vec r')C(\vec r,\vec r')dl' - \int_\Gamma \psi(\vec r')D(\vec r,\vec r')dl' = 0, \qquad (2)$$

978-1-4244-7045-7/10/$26.00 ©2010 IEEE

where dl' is the element of the arc on Γ, $\varphi(\vec{r}) = U_i(\vec{r})$ and $\psi(\vec{r}) = \partial U_i(\vec{r})/\partial n, \quad \vec{r} \in \Gamma$.

Here, the kernel functions are

$$A(\vec{r},\vec{r}\,') = \partial G_i(\vec{r},\vec{r}\,')/\partial n' - \partial G_e(\vec{r},\vec{r}\,')/\partial n',$$

$$B(\vec{r},\vec{r}\,') = G_i(\vec{r},\vec{r}\,') - \eta_i/\eta_e G_e(\vec{r},\vec{r}\,') \tag{3}$$

$$C(\vec{r},\vec{r}\,') = \partial^2 G_i(\vec{r},\vec{r}\,')/\partial n \partial n' - \partial^2 G_e(\vec{r},\vec{r}\,')/\partial n \partial n',$$

$$D(\vec{r},\vec{r}\,') = \partial G_i(\vec{r},\vec{r}\,')/\partial n - (\eta_i/\eta_e)\partial G_e(\vec{r},\vec{r}\,')/\partial n \tag{4}$$

Note that the kernel functions $A(t,\tau)$ and $D(t,\tau)$ are continuous, and the kernel functions $B(t,\tau)$ and $C(t,\tau)$ have logarithmic singularities.

IV. Discretization of Integral Equations

One of the most efficient discretization techniques is the method of quadratures, also known as the Nystrom method [6]-[8]. This latter method is based on the replacement of the integrals with approximate sums using the appropriate quadrature formulas. As some of the kernel functions have logarithmic singularities, it is convenient to represent all of the kernels in (3) and (4) in such a way that these singularities are extracted [7],[8]. Then the integrals are approximated by two different quadrature rules for the regular and singular parts with the same equidistant set of points $t_p = \pi p/N$, $p = 0,1,...,2N-1$. Namely, we use a trigonometric quadrature rule for the parts with logarithmic singularities and a trapezoidal rule for the regular parts [5]. By evaluating the integrals from (1) for each $t = t_s$ with the aid of the quadrature rules, we obtain a determinantal equation for the eigenvalues. A secant-type iterative method [2] is further used to find the eigenvalues numerically from this equation.

V. Numerical Results

For simplicity, we consider the kite contour as a continuous deformation of the circle, and therefore denote the modes of the kite cavity using the notations of their limiting forms in the circle with a prefix "quasi". In Fig. 2, we present the dependences of the lasing frequency and threshold gain of the doublet of low-order modes quasi-H_{21} on the kite contour deformation parameter, δ. The initial values of thresholds of these modes are quite high. If δ gets larger, the frequencies of both modes grow up. Unlike this, only one of the modes (odd with respect to the x-axis) has the threshold that grows up monotonically while another (even mode) displays a maximum of threshold around $\delta = 0.3$.

The shape of the far-field radiation pattern changes very dramatically with the growth of δ. In Fig. 3, the patters of the modes quasi-H_{21} are shown for the maximum value of δ of the studied range, i.e. $\delta = 0.5$. As visible, the directivity can be both larger and smaller than the circular-cavity value 2.

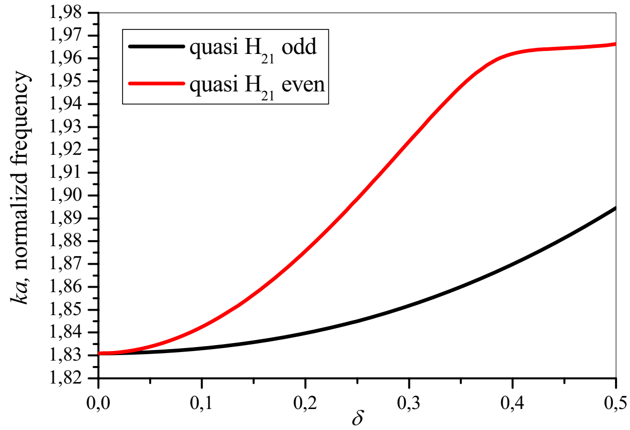

(a)

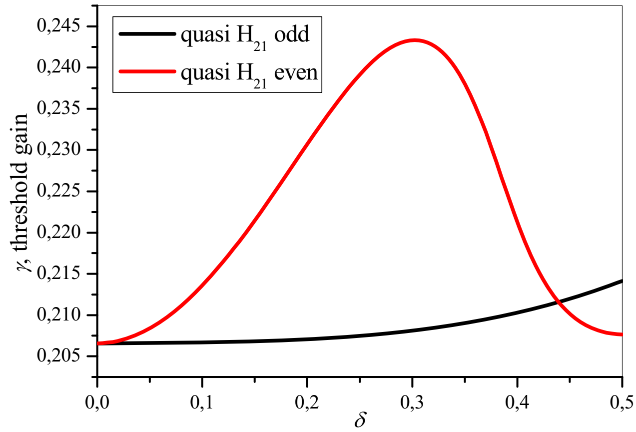

(b)

Fig. 2. Normalized lasing frequency (a) and threshold gain (b) as a function of the kite deformation parameter δ, for the doublet of quasi-$H_{2,1}$ modes, $\alpha = 2.63$, $N = 50$

In Fig. 4, presented are the lasing frequencies and thresholds for the doublet of modes quasi-H_{51} that display the features of the whispering-gallery modes at $\delta = 0$. Their initial thresholds are some 10 times lower than those of the quasi-H_{21} modes.

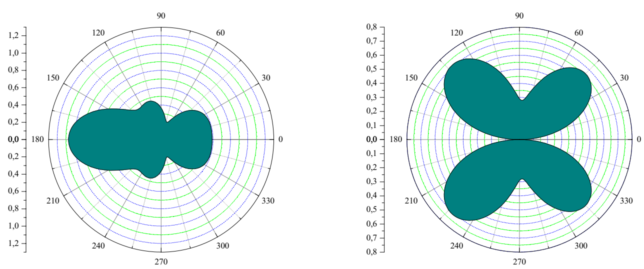

(a) (b)

Fig. 3. Normalized far-field emission patterns for $\delta = 0.5$, $\alpha = 2.63$, and $N = 50$: (a) quasi-$H_{2,1}$ even, directivity = 3.43; (b) quasi-$H_{2,1}$ odd, directivity = 1.98.

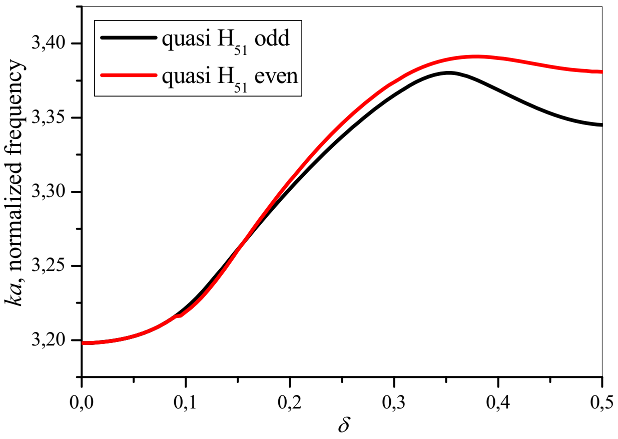

(a)

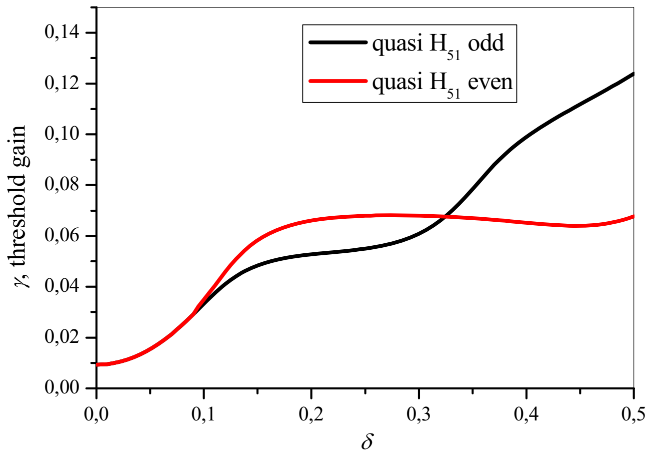

(b)

Fig. 4. The same as in Fig. 2 however for the modes quasi-H_{51}.

The even-type mode of this doublet also show a maximum threshold value around $\delta = 0.2$. In Fig. 5, the far-field patters of the modes quasi-H_{51} are shown for $\delta = 0.5$. As visible, at such deformation their directivities are larger than for the low-order modes quasi-H_{21}. Note that the number of emission lobes is no more the same as in the circular cavity.

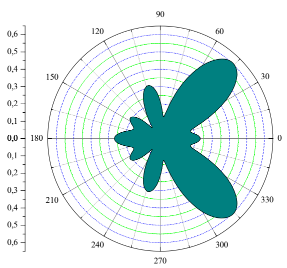

(a)

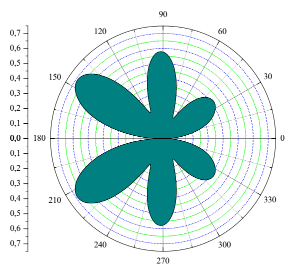

(b)

Fig. 5. The same as in Fig. 2 however for the modes (a) quasi-H_{51} even, directivity = 3.71; (b) quasi-H_{51} odd, directivity = 2.74

VI. Conclusions

We have presented preliminary results of the LEP-based numerical analysis of the lasing modes in the 2-D model of a kite-shaped thin microcavity laser. This shape is attractive as it enables one to study the variations of the near and far-field modal patterns, and also the lasing frequencies and threshold gains for a variety of shapes changing smoothly from a circle to a "boomerang" cavity. As one can see, even small deformations of this sort can lead to considerable changes of the emission patterns and thus provide greater directivities.

Acknowledgments

This work was supported in part by the National Academy of Sciences of Ukraine via the Young Scientist Scholarship to the first author, the European Science Foundation via research network "Newfocus", and the Ministry of Education and Science, Ukraine via project M/146-2010.

References

[1] E.I. Smotrova, A.I. Nosich, "Mathematical study of the 2D lasing problem for the whispering-gallery modes in a circular dielectric microcavity," *Optical and Quantum Electronics*, 2004, vol. 36, no 1-3, pp. 213-221.

[2] E.I. Smotrova, *et al.*, "Cold-cavity thresholds of microdisks with uniform and non-uniform gain: quasi-3D modelling with accurate 2D analysis," *IEEE J. Selected Topics Quant. Electron.*, vol. 11, pp. 1135-1142, 2005.

[3] E.I. Smotrova, et al., "Ultralow lasing thresholds of the pi-type supermodes in cyclic photonic molecules composed of sub-micron disks with monopole and dipole modes," *IEEE Photonics Technology Letters*, vol. 18, no 19, pp. 1993-1995, 2006.

[4] E.I. Smotrova, *et al.*, "Lasing frequencies and thresholds of the dipole-type supermodes in an active microdisk concentrically coupled with a passive microring," *J. Opt. Society America A*, vol. 25, no 11, pp. 2884-2892, 2008.

[5] E.I. Smotrova, *et al.*, "Optical fields of the lowest modes in a uniformly active thin sub-wavelength spiral microcavity," *Optics Letters*, vol. 34, no 24, pp. 3773-3775, 2009.

[6] L. Wang, J.A. Cox, A. Friedman, "Modal analysis of homogenious optical waveguides by the boundary integral formulation and the Nyström method," *J. Opt. Soc. Am. A*, vol. 15, no. 1, pp.92-100, 1998.

[7] D. Colton, R. Kress, *Inverse Acoustic and Electromagnetic Scattering Theory*, Springer, Berlin, 1998.

[8] J. Tsalamengas, "Exponentially converging Nystrom methods applied to the integral/integro-differential equations of oblique scattering hybrid wave propagation in presence of composite cylinders of arbitrary cross section," *IEEE Trans. Antennas Propag.*, vol. 55, no 11, pp. 3239-3250, 2007.